INSIGHT INTO FORMATION PROCESSES OF LAYERED EJECTA CRATERS ON MARS FROM THERMOPHYSICAL OBSERVATIONS. R. H. Hoover[1,2,⌘] S. J. Robbins[1], N. E. Putzig[3], J. D. Riggs[4], B. M. Hynek[2]. [1]Southwest Research Institute, 1050 Walnut St., Suite 300, Boulder, CO 80302, USA; [2]University of Colorado, Boulder, CO; [3]Planetary Science Institute, Lakewood, CO; [4]Northwestern University, Chicago, IL. ⌘RHoover@Boulder.SwRI.edu

Synopsis: Understanding the morphological characteristics of craters that are indicative of their formation environment can provide insight into surface geology. Specifically, layered ejecta (LE) craters, found on Mars [e.g 1] and some other planetary bodies [e.g. 2,3,4] have been hypothesized to have formed as a result of either interactions with subsurface volatiles (volatile fluidization model) [e.g 5,6] or with the atmosphere (atmospheric entrainment model) [e.g 7,8]. Formation of LE craters by either model should result in different grain size distributions throughout the ejecta deposit. Using thermal inertia to infer surface properties, we investigated LE craters and their ejecta deposits in an effort to distinguish between possible LE formation processes on Mars. Thermophysical properties of crater ejecta are used to determine grain size distribution, to model horizontal mixtures and vertical layering, and to identify materials present within the ejecta. We assessed the thermal properties of 50 globally distributed LE craters (Figure 1) using Mars Odyssey Thermal Emission Imaging System (THEMIS) [9] and Mars Global Surveyor Thermal Emission Spectrometer (TES) [10] data.

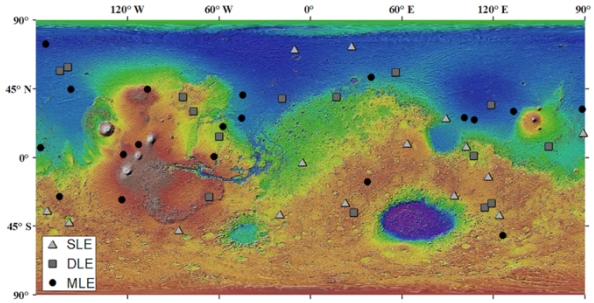

Figure 1: Global topographic map of Mars from MOLA data displaying the distribution of Single-, Double- and Multi-layered ejecta (SLE, DLE and MLE) craters selected for investigation in this study.

Layered Ejecta Craters: Two primary hypotheses exist to explain the formation of layered ejecta craters. The first hypothesis is the "fluidized model" in which an impactor strikes a volatile-rich surface resulting in the melting or vaporization of volatiles [5,6]. The volatiles become entrained in the ejecta causing it to flow and act like a fluid [5,6]. The second hypothesis is the "atmospheric model" in which the ejecta of a crater interacts with the atmosphere [7,8]. Each model has implications for the geology and environment of the impacted area. For example, the fluidized model implies the presence of subsurface volatiles during crater formation.

Grain size distributions within the crater ejecta are predicted to be different for each model. For the atmospheric entrainment model the largest grains within the ejecta deposits would be located nearest the crater rim, and finer-grained sediment would be entrained in the atmosphere and emplaced farther from the rim [7,8]. For the volatile fluidization model larger grains and boulders would be located near the ejecta terminus [5]. Thus, investigating the thermophysical properties of the crater ejecta to identify the distribution of grain size is one potential means to distinguish between these two models.

Methods: The apparent thermal inertia (ATI) of a surface is derived from individual surface or brightness temperatures obtained by TES and THEMIS. Values derived from TES, with a 3 km/pixel scale, are used to identify large-scale heterogeneities by examining their diurnal and seasonal variations and comparing them to values calculated for two-component heterogeneity models created for a variety of materials (e.g., dust, sand, rock/ice, duricrust) with either horizontal mixing or vertical layering representing the top few cm of the surface [11]. Values derived from THEMIS data, with 100 m/pixel scale, are used to identify trends and variations within the crater ejecta to further clarify the near-surface materials at finer lateral resolution [12]. Useful THEMIS images for thermal analysis are largely limited to nighttime observations because the majority of daytime observations are too close to dusk to provide accurate thermal inertia results [12].

Results: Several different characteristic patterns in the THEMIS data for ejecta deposits of LE craters emerged from our analysis of THEMIS data and we divided these patterns into five classes. A summary of each THEMIS class type is discussed in Table 1 and associated examples are shown in Figure 2. For our TES analysis, 23 craters matched currently available two-later heterogeneity models, 19 models did not match current models, and the remaining 8 were eliminated from analysis due to resolution contraints. A summary of model matches to specific crater type is shown in Table 2.

Table 1: Description of each identified THEMIS class type and associated Figure.

Class	Description	# of craters	Corresponding Figure
1	ATI of ejecta deposit is greater than that of surroundings	8	**Error! Reference source not found.**a
2	ATI of ejecta deposit is less than that of surroundings	3	**Error! Reference source not found.**b
3	Edge of ejecta has greater ATI than that of surroundings	12	**Error! Reference source not found.**c
4	Edge of ejecta deposit has less ATI than that of surroundings	3	**Error! Reference source not found.**d
5	ATI of ejecta deposit is same as that of surroundings or no distinct pattern found	13	**Error! Reference source not found.**e

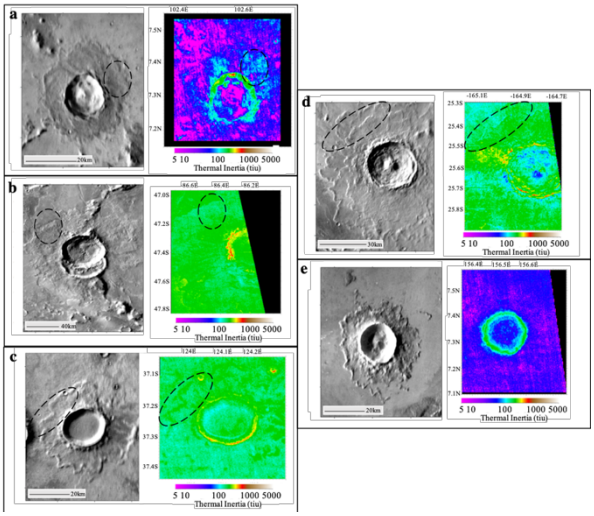

Figure 2: Examples of each THEMIS Class. Dashed circles indicate areas representative of the chracteristics associated with each THEMIS class type

Table 2: Summary of two-material heterogeneity models matching TES ATI results for single-, double-, and multi-layered ejecta craters (SLE, DLE, and MLE, respectively)

TES Model	SLE	DLE	MLE	Total
Crust over dust	3	1	3	7
Dust over crust	1	1	1	3
Dust over rock	1	1	3	5
Sand over rock	2	0	0	2
Dust-crust mix	1	0	1	2
Dust-rock mix	0	3	1	4
Inconclusive	4	6	9	19

Discussion: Each THEMIS ATI class provides information with potential implications for the formation processes and target materials of at least some LE craters. Overall, 12 craters exhibit characteristics consistent with the volatile fluidization model, 2 craters exhibit characteristics consistent with the atmospheric entrainment model, 3 craters exhibit characteristics that fit both the volatile fluidization and atmospheric entrainment models, while 22 craters do not have characteristics supporting either model, based on our hypotheses. Our TES anlysis identifies several craters that provide evidence in support of the volatile fludization model. Eleven craters exhibit characteristics matching that of a rock/ice thermal signature, but no trends were observed between identification and crater type. Although we state that the presence of subsurface ground ice would support the volatile fluidized model, we recognize that the current state of volatiles does not necessarily represent the presence of volatiles during crater formation. Simultaneously, the lack of identification in some cases fails to indicate the absence of subsurface water ice currently (i.e., it may be present but not detected below ~2 seasonal thermal skin depths of overlying material) or in the past at the time of the impact event.

Conclusions: THEMIS analysis of small-scale heterogeneities within the crater ejecta did not provide overhwleming evidence of consistent and significant correlations to types of LE craters. Additionally, our TES analysis also provided equivical results. While thermal patterns may exist within an individual ejecta deposits, a trend among LE crater types was not observed. This lack of a consistent thermal trend may be a result of the significant influence of dust cover, which is potentially associated with the crater degradation state or other post-formation processes. Future work aimed at determining the formation mechanisms of LE craters should include different datasets such as radar sounding data (Bain et al., this conference).

References: [1] McCauley (1973) JGR, 78, 20. [2] Maloof et al. (2010) doi: 10.1130/B26474.1. [3] Horner and Greeley (1982) Icarus, 51, 3. [4] Boyce et al., (2010) doi.org/10.1111/j.1945-5100.2010.01044.x. [5] Carr, M. H. (1977) JGR, 82, 28. [6] Mouginis-Mark (1979) JGR, 84, B14. [7] Schultz and Gault (1979) JGR, 84, B13. [8] Schultz (1992) JGR, 97, E7. [9] Christensen et al. (2004) Space Science Reviews, 110, 85-13. [10] Christensen et al. (2001) JGR, 106, E10. [11] Mellon, M. T. et al. (2000) Icarus, 148, 437-455. [12] Putzig, N. E. and Mellon, M. T. (2007) Icarus, 191, 52-67.

Funding: This work was supported by NASA's Mars Data Analysis Program.